RESEARCH ARTICLE

JBMR®

Increased Bone Volume by Ixazomib in Multiple Myeloma: 3-Month Results from an Open Label Phase 2 Study

Marta Diaz-delCastillo,[1] Michael Tveden Gundesen,[2,3] Christian Walther Andersen,[4] Anne Lerberg Nielsen,[4] Hanne Elisabeth Højsgaard Møller,[5] Pernille Just Vinholt,[6] Jon Thor Asmussen,[7] Ida Bruun Kristensen,[2,8] Charlotte Guldborg Nyvold,[8] Niels Abildgaard,[2,3] Thomas Levin Andersen,[1,3,5] and Thomas Lund[2,3]

[1]Department of Forensic Medicine, Aarhus University, Aarhus, Denmark
[2]Department of Hematology, Odense University Hospital, Odense, Denmark
[3]Department of Clinical Research, University of Southern Denmark, Odense, Denmark
[4]Department of Nuclear Medicine, Odense University Hospital, Odense, Denmark
[5]Department of Pathology, Odense University Hospital, Odense, Denmark
[6]Department of Clinical Biochemistry, Odense University Hospital, Odense, Denmark
[7]Department of Radiology, Odense University Hospital, Odense, Denmark
[8]Hematology-Pathology Research Laboratory, Research Unit for Hematology & Research Unit for Pathology, University of Southern Denmark & Odense University Hospital, Odense, Denmark

ABSTRACT

Multiple myeloma (MM) is an incurable bone marrow cancer characterized by the development of osteolytic lesions due to the myeloma-induced increase in osteoclastogenesis and decrease in osteoblastic activity. The standard treatment of MM often involves proteasome inhibitors (PIs), which can also have a beneficial off-target bone anabolic effect. However, long-term treatment with PIs is unadvised due to their high side-effect burden and inconvenient route of administration. Ixazomib is a new-generation, oral PI that is generally well tolerated; however, its bone effect remains unknown. Here, we describe the 3-month results of a single-center phase II clinical trial investigating the effect of ixazomib treatment on bone formation and bone microstructure. Thirty patients with MM in stable disease not receiving antimyeloma treatment for ≥3 months and presenting ≥2 osteolytic lesions received monthly ixazomib treatment cycles. Serum and plasma samples were collected at baseline and monthly thereafter. Sodium ^{18}F-Fluoride positron emission tomography (NaF-PET) whole-body scans and trephine iliac crest bone biopsies were collected before and after three treatment cycles. The serum levels of bone remodeling biomarkers suggested an early ixazomib-induced decrease in bone resorption. NaF-PET scans indicated unchanged bone formation ratios; however, histological analyses of bone biopsies revealed a significant increase in bone volume per total volume after treatment. Further analyses of bone biopsies showed unchanged osteoclast number and *COLL1A1*^{High}-expressing osteoblasts on bone surfaces. Next, we analyzed the superficial bone structural units (BSUs), which represent each recent microscopic bone remodeling event. Osteopontin staining revealed that following treatment, significantly more BSUs were enlarged (>200,000 μm^2), and the distribution frequency of their shape was significantly different from baseline. Overall, our data suggest that ixazomib induces overflow remodeling-based bone formation by decreasing the level of bone resorption and promoting longer bone formation events, making it a potentially valuable candidate for future maintenance treatment. © 2023 The Authors. *Journal of Bone and Mineral Research* published by Wiley Periodicals LLC on behalf of American Society for Bone and Mineral Research (ASBMR).

KEY WORDS: BONE HISTOMORPHOMETRY; TUMOR-INDUCED BONE DISEASE; OSTEOBLASTS; OSTEOCLASTS; ANABOLICS

Received in original form December 2, 2022; revised form March 16, 2023; accepted March 21, 2023.

Address correspondence to: Marta Diaz-delCastillo, PhD, Department of Forensic Medicine, University of Aarhus, Denmark, Palle Juul-Jensens Blvd. 99, DK 8200 Aarhus. E-mail: marta@forens.au.dk

Additional Supporting Information may be found in the online version of this article.

Marta Diaz-delCastillo and Michael Tveden Gundesen shared first authors.

Thomas Levin Andersen and Thomas Lund shared last authors.

Journal of Bone and Mineral Research, Vol. 38, No. 5, May 2023, pp 639–649.

DOI: 10.1002/jbmr.4807

Introduction

Multiple myeloma (MM) is an incurable malignant plasma cell disease associated with overproduction of monoclonal immunoglobulin (M-protein), suppression of normal immunoglobulin synthesis, kidney and bone marrow failure, hypercalcemia, and skeletal destruction.[1] While the disease remains incurable, overall survival has improved significantly with the introduction of novel therapies, such as immune modulating drugs,[2] proteasome inhibitors (PIs),[3] and the anti-CD38 antibody daratumumab.[4] Despite developments in disease management, bone disease remains a major concern.[5] Indeed, patients with MM report more symptoms and problems than patients with other hematological cancers such as leukemia or lymphoma,[6] and the risk of early disability pension in MM is more than twice that of other malignant hematological diseases.[7]

Bone destruction is the hallmark of MM, with up to 79% of patients presenting osteolytic bone lesions or fractures at diagnosis and more than 60% complaining of bone pain.[5,8] Bone damage in patients with MM is caused by a constellation of bone marrow microenvironmental alterations, including the myeloma-induced upregulation of receptor activator of nuclear factor kappa B ligand (RANKL). This results in increased recruitment and activation of the bone resorbing osteoclast cells,[9,10] as well as the upregulation of interleukin-6 (IL-6) and Dickkopf-related protein 1 (DKK1), which plays an important role in myeloma bone disease by inhibiting osteoblast recruitment and differentiation and the consequent bone formation.[11,12] Altogether, MM induces increased bone resorption and decreased bone formation, leading to an imbalance in the normal bone remodeling process that results in the development of focal osteolytic lesions. Importantly, the myeloma-induced impairment in bone remodeling remains even in stable disease. To prevent skeleton-related events, bisphosphonates or denosumab are considered the gold standard in MM and administered independently of antineoplastic treatment.[13] However, their efficacy is limited, and they can cause a variety of side effects upon long-term use, including osteonecrosis of the jaw and suppression of bone turnover, leading to increased fracture risk and rebound bone loss when using denosumab.[13-15]

It was first reported in 2005 that the PI bortezomib could have an osteoblastic stimulatory effect, as responding patients in bortezomib treatment displayed increased bone-specific alkaline phosphatase (bALP).[16,17] Later, multiple studies confirmed the anabolic bone effect of bortezomib through bone histomorphometry and micro–computed tomography (μCT).[18,19] Similar bone effects have been observed in patients receiving carfilzomib treatment, suggesting a potential bone anabolic class effect of PI.[20] However, long-term treatment with either bortezomib or carfilzomib is challenging due to their route of administration (subcutaneous or intravenous, respectively) and the high risk of serious side effects, such as peripheral neuropathy and cardiac toxicity.

Ixazomib is a new-generation PI that can be administered orally and is generally well tolerated; moreover, ixazomib treatment has shown efficacy in prolonging progression-free survival (PFS) when administered as a single agent,[21,22] making it an attractive alternative for long-term treatment of patients with MM. However, the potential effect of this second-generation PI on myeloma-induced bone disease remains unknown. This study investigates the potential bone anabolic effect after three full 28-day cycles of ixazomib treatment in a phase 2 open-label clinical study on patients with stable MM.

Materials and Methods

Study design and endpoints

This is a prospective, single-center, interventional, open-label, phase 2 clinical study investigating the bone effect of ixazomib treatment in patients with MM (ClincalTrials.gov: NCT04028115). Patients were included at Odense University Hospital (Denmark) after approval from the Regional Committees on Health Research Ethics for Southern Denmark (S-20190043; July 4, 2019) and conducted according to the Helsinki Declaration. Patients were included upon collection of informed consent between August 2019 and August 2021. Inclusion criteria were set to patients with symptomatic MM in stable disease not receiving antimyeloma treatment for ≥3 months and presenting detectable osteolytic disease with ≥2 osteolytic lesions at least 5 mm in diameter; detailed inclusion and exclusion criteria are described in Table S1.

Included patients received ixazomib treatment in standard dosing (4 mg) orally on days 1, 8, and 15 in a 28-day cycle, as previously described,[21] for up to 24 cycles; delay of up to 1 week before starting next treatment cycle was accepted. All patients were treated with acyclovir from the trial start to reduce the risk of herpes zoster reactivation; treatment is scheduled to continue for ≥2 months after end of study. A medical doctor evaluated the patients once per 4-week treatment cycle to record adverse effects (AEs), performance, and medicine status. AEs were graded in accordance with Common Terminology Criteria for AE (CTCAE version 4.0). All nonhematological AEs should be reduced to baseline or grade ≤1 before starting the next treatment cycle. Neutrophils $\geq 1.0 \times 10^9$/L and platelets $\geq 75 \times 10^9$ were required for new cycle initiation. If treatment was paused ≥2 weeks due to AEs, the next cycle resumed with a reduced dose. The following doses were used: start dose 4 mg, reduced dose (level 1) 3 mg, reduced dose (level 2) 2.3 mg; no further dose reductions were permitted. Patients received zoledronic acid as part of their normal standard of care (further details can be found in Table 1). No patients were treated with denosumab.

The primary endpoint was to determine healing of osteolytic lesions on low-dose CT after 24 months compared with baseline. Secondary endpoints included (i) increased bone formation in NaF-PET scans after 3, 12, and 24 months of treatment compared with baseline; (ii) increased bone anabolism measured as increased levels of procollagen type 1 N-terminal propeptide (P1NP), bALP, and osteocalcin (OC) in monthly serum samples compared with baseline; (iii) increased ratio of bone formation to resorption as measured by bone formation serum markers P1NP, bALP, and OC and bone resorption serum markers C-terminal telopeptide (CTX) and tartrate-resistant acid phosphatase 5b (TRAcP5b) after 3, 12, and 24 months, compared with baseline; and (iv) increased bone formation assessed by histomorphometry on bone biopsies collected at baseline and after 3, 12, and 24 months of treatment.

Sodium^{18}Fluoride-positron emission tomography (NaF-PET) whole-body scans

CT (Discovery 690, 710 Ge Medical Systems, Wisconsin, USA) scan was performed with a tube voltage of 120 kV and variable tube current by a noise index of 35 on a 40-mm detector

Table 1. Baseline Characteristics of 30 Patients Enrolled in This Phase 2 Study

Variable	Measure
Age (median, range; years)	58.29 (38–76)
Sex (*N*, %; male)	14 (46.67)
BMI (median, range; kg/m^2)	26.84 (20.98–37.84)
Myeloma type (*N*, %)	
IgG	17 (56.66)
IgG kappa	12 (70.59)
IgG lambda	5 (29.41)
IgA	3 (10.00)
IgA kappa	3 (100.00)
IgE	1 (3.33)
IgE kappa	1 (3.33)
Light chain	8 (26.67)
Light chain kappa	7 (87.50)
Light chain lambda	1 (12.50)
Nonsecretory	1 (3.33)
ISS (N, %)	
ISS 1	15 (50.00)
ISS 2	7 (23.33)
ISS 3	8 (26.67)
R-ISS (*N*, %)	
R-ISS 1	7 (23.33)
R-ISS 2	16 (53.33)
R-ISS 3 N/A	5 (16.67) 1 (3.33)
Number of lines of treatment (*N*, %)	
1 line	16 (53.33)
2 lines	8 (26.67)
3 lines	5 (16.67)
4 or more lines	1 (3.33)
Previous zoledronic acid treatment	
Previous treatment (*N*, %)	29 (96.67%)
Number of doses at baseline (average; min-max)	19.59 (0–48)

configuration. Two axial reconstructions were done: 3.75-mm slices with a "Stnd" kernel and 1.25-mm slices with "Bone" kernel; the latter was used for sagittal and coronal 3-mm reformats on the scanner. Images were evaluated using GE AW-server version 3.2 diagnostic software.

For the PET acquisition, patients were injected with 200 MBq ^{18}F-labeled sodium fluoride (NaF) and scanned after resting for 30 minutes. The PET signal was acquired in 1-minute frames with an overlap of 50% between them. Discovery MI scanners are equipped with digital detectors capable of time-of-flight reconstruction, and images were reconstructed iteratively (four iterations and 17 subsets) as well as with the Q.Clear algorithm.

Blood analyses

TRACP5b and bALP were measured in serum, and CTX-1, P1NP, and OC in K2-EDTA plasma. Analyses were performed on an IDS-iSYS Multi-Discipline Automated System (Immunodiagnostic Systems Holdings, UK) according to the manufacturer's instructions.

Bone biopsies

Needle bone biopsies (3 mm in diameter) from the iliac crest were fixed in buffered 4% paraformaldehyde, decalcified in buffered 0.5 M EDTA with 0.4% paraformaldehyde, and embedded in paraffin. Bone biopsies were serially sectioned at 3.5-µm thickness; one section from each biopsy underwent duplex in situ hybridization for *COL1A1* and TRAcP5b immunostaining, and another was immunostained for osteopontin (OPN).

In situ hybridization

Sections were deparaffinized in xylene and ethanol and pretreated in RNAscope Target Retrieval (Advanced Cell Diagnostics, Hayward, CA, USA) solution for 15 minutes at 85°C and in 10% pepsin for 20 minutes at 40°C. Sections were hybridized overnight at 40°C with a 20-basepair probe targeting the 711–1682 nucleotide region of *COL1A1* mRNA (NM_006080.2). Signal amplification followed manufacturer's recommendations in a HybEZTM hybridization oven (Advanced Cell Diagnostics, Hayward, CA, USA) and was visualized with a teal kit (Roche, Pleasanton, CA, USA). Sections were then blocked 20 minutes in 5% casein/TBS and incubated for 30 minutes with a mouse monoclonal antibody against TRACP5b (Millipore BABF96; AB_10845145). Upon 10 minutes of blocking in 3% H_2O_2/TBS, the antibody was labeled with peroxidase-conjugated anti-mouse IgG polymers for 30 minutes (BrightVision, Duiven, Holland) and Deep Space Black (DSB; Biocare, Concord, MA, USA). Slides were counterstained with Mayer's hematoxylin and mounted with Aquatex (Merck Millipore, Darmstadt, Germany). Negative controls were performed by omission of primary antibody/target probe.

Immunostaining

Sections were deparaffinized in xylene and ethanol, incubated overnight in TE buffer (pH 9.0) at 60°C, blocked with 5% casein/Tris-buffered saline (TBS), and incubated first with avidin and then biotin for 10 minutes. A biotinylated goat anti-OPN antibody (1:1000; R&D systems, BAF1433; AB_355994) was added for 2 hours, followed by alkaline-phosphatase-conjugated streptavidin (Merck Millipore, Darmstadt, Germany) and Liquid Permanent Red (DAKO, Glostrup, Denmark). Sections were counterstained with Mayer's hematoxylin and mounted with Aquatex (Merck Millipore, Darmstadt, Germany). Negative controls were performed by omission of primary antibody.

Histomorphometric assessment

Bone slides were ×20 brightfield scanned in the high-throughput VS200 slide scanner (Olympus Microscopy, Tokyo, Japan) and analyzed through a combination of machine learning and manual quantification with VS200 Desktop and Deep Neuronal Network (Olympus). Regions of interest were defined to exclude borders and detached tissue within the in situ hybridized sections as well as endocortical bone within the OPN-immunostained sections. Four histological samples were excluded from further analyses due to insufficient tissue quality.

The bone surface (BS), *COL1A1*^{high} osteoblasts, and TRACP$^+$ osteoclasts present in in situ hybridization slides were automatically detected with an optimized neuronal network. Detected osteoclasts and osteoblasts were visually confirmed to validate cell lineage. The percentage of BS covered by *COL1A1*^{high} osteoblasts (*COL1A1*^{high} Ob.S/BS) and number of osteoclasts per BS (Oc.N/BS) were calculated.

Trabecular bone volume (BV/TV) was automatically detected in OPN-immunostained slides using an optimized neuronal network. The size, shape, and appearance of recently formed bone

structural units (BSUs) within the trabecular bone were investigated in the same sections, as in our previous study.[23] Briefly, all BSU profiles (BSU.Pf.) presenting one or more surfaces adjacent to the marrow space without signs of further alteration by posterior remodeling events were manually outlined and categorized as "superficial BSU.Pf." (BSU^{SUP}.Pf.). The following size and shape parameters were analyzed for each individually measured BSU^{SUP}.Pf.: (i) area (BSU^{SUP}.Pf.Ar.); (ii) circularity (BSU^{SUP}.Pf.Cir.): squared quotient of width and length, where 1 indicates full circle; (iii) aspect ratio (BSU^{SUP}.Pf.A.R.): maximum ratio between length and width of bounding box; (iv) shape factor (BSU^{SUP}.Pf.Sh.F.): area relative to area of circle of equal perimeter; (v) solidity (BSU^{SUP}.Pf.Sol.): area relative to area of BSU's convex hull; and (vi) width (BSU^{SUP}.Pf.Wi.): distance between two boundary points on line contained within BSU that crosses its center of mass.

Next, we performed a detailed characterization of the BSU^{SUP}.Pf. measuring an area ≥ 200,000 μm (enlarged BSU^{SUP}.Pf.). To elucidate whether the enlarged BSU^{SUP}.Pf. originated from bone modeling or remodeling events, their OPN^{rich} cement lines of origin were classified as quiescent (smooth lines parallel to defined lamella structures) or eroded (scalloped lines cutting through the lamella present underneath). Enlarged BSU^{SUP}.Pf. were then scored according to their historical bone growth as follows: (i) new BSU^{SUP}.Pf.: completely superficial, that is, presenting no additional layers of bone growth toward marrow; (ii) parent BSU^{SUP}.Pf.: presenting one layer of subsequential bone growth toward marrow; and (iii) grandparent BSU^{SUP}.Pf.: presenting ≥2 layers of superficial bone growth toward marrow. To determine whether bone formation was still ongoing at the time the biopsy was collected, enlarged BSU^{SUP}.Pf. were classified as containing osteoid-covered BSs or not. Moreover, to estimate the extent of bone formation, the number of trabecular rods embedded within each enlarged BSU^{SUP}.Pf. was quantified. Finally, each individual enlarged BSU^{SUP}.Pf. was classified according to whether they contained any extent of woven bone, identified as disorganized lamella. Stained histological sections were assigned a random code, and pseudo-anonymized tissue was analyzed by the same investigator, who was blinded to patient identity and experimental group, to minimize bias.

Statistical analyses

Power calculations on the primary outcome are hindered by the exploratory nature of the study, as only case reports previously addressed bone healing during PI treatment. However, in the VISTA trial reported by Delforge et al.,[24] 63% (7/11) of patients showed radiological signs of bone healing following antimyeloma treatment. Thus, inclusion of 30 patients in this trial was expected to yield a confidence interval of ±17.9% with a 95% margin of error.

Data were plotted in GraphPad Prism version 9.3.1 (GraphPad, La Jolla, CA, USA) and analyzed by two-tailed Student's *t*-test, chi-squared (ie, contingency graphs), or mixed-effects one- or two-way ANOVA, as appropriate. Serum sample data passed D'Agostino and Pearson's normality test ($p > 0.05$). Clinical parameters confounding treatment-induced changes in BV were explored by multiple linear regression, where age, sex, body mass index (BMI), and revised international staging system (R-ISS) were considered independent variables. Data are presented as individual values in box plots and superimposed mean ± standard deviation (SD), or for serum markers and ratios, as mean ± SD.

Results

Patient enrolment

Thirty-four patients were invited to participate and underwent imaging evaluation for potential study enrolment; four patients were excluded before enrollment due to patient wishes to minimize hospital exposure during the COVID-19 pandemic ($n = 1$), other cancer found in screening imaging ($n = 1$), insufficient kidney function ($n = 1$), and insufficient bone damage according to inclusion criteria ($n = 1$). All 30 included patients completed the first three cycles of ixazomib treatment; patient characteristics at diagnosis can be found in Table 1. None of the patients had received denosumab treatment. Twenty-nine patients (97%) had received zoledronic acid before study enrollment, 19 patients (63.33%) received an additional dose of zoledronic acid at baseline, and 18 (60.00%) continued bisphosphonate treatment throughout the first three cycles of ixazomib. Zoledronic acid (iv) was administered every fourth week at a dose of 4 mg for patients with an eGFR >60 and 3 mg for patients with an eGFR between 30 and 60.

Ixazomib treatment induces fast reduction in bone resorption without affecting bone formation markers

Thirty patients with stable MM received three full 28-day cycles of oral ixazomib treatment; serum and plasma samples were collected monthly upon completion of each treatment cycle. Ixazomib treatment significantly decreased serum TRACP5b and CTX already after 1 or 2 months of treatment, respectively, compared with baseline (Fig. 1*A*); no significant changes in serum levels of bone formation markers P1NP and bALP were observed (Fig. S1). Likewise, the ratios of serum bone biomarkers remained unchanged, except for a significant decrease of TRACP5b/bALP ratio after 2 months of treatment (Fig. S1).

NaF-PET scans and trephine iliac crest biopsies were collected at baseline and upon completion of the three treatment cycles. CT scans showed unchanged osteosclerotic lesions (data not shown). Similarly, NaF-PET scans from skull, sternum, vertebrae, pelvis, and femur showed unchanged mean standard uptake values (SUV) after 3 months of treatment (Fig. 1*B* and Fig. S1). Among all patients, a total of 87 osteolytic lesions were detected, mainly localized in the vertebrae (31%), pelvis (26%), sternum (17%), and skull (12%). Focal osteolytic lesions were discovered less frequently in the femur (3.5%), humerus, dens axis and scapula (2.3%), and ribs and shoulders (1.2%). While the max SUV measured in osteolytic lesions at each skeletal site remained unchanged after treatment, the combined maximum SUV significantly decreased after three treatment cycles (Table S2).

Needle bone biopsies from the iliac crest were in situ hybridized for *COL1A1*, in combination with TRACP5b immunostaining (Fig. 1*C*); results were analyzed through a combination of machine learning and manual quantification. No significant differences in $COL1A1^{high}$ Ob.S/BS were detected in any bone compartment (endocortical or trabecular bone) or in the total bone section (Fig. 1*D*). Neither surface nor detached Oc.N/BS was significantly different after three ixazomib cycles compared with baseline (Fig. 1*D*). Overall, these results suggest that ixazomib promotes a decrease in bone resorption without affecting the number of osteoclastic profiles, the extent of bone-forming osteoblasts, or bone formation.

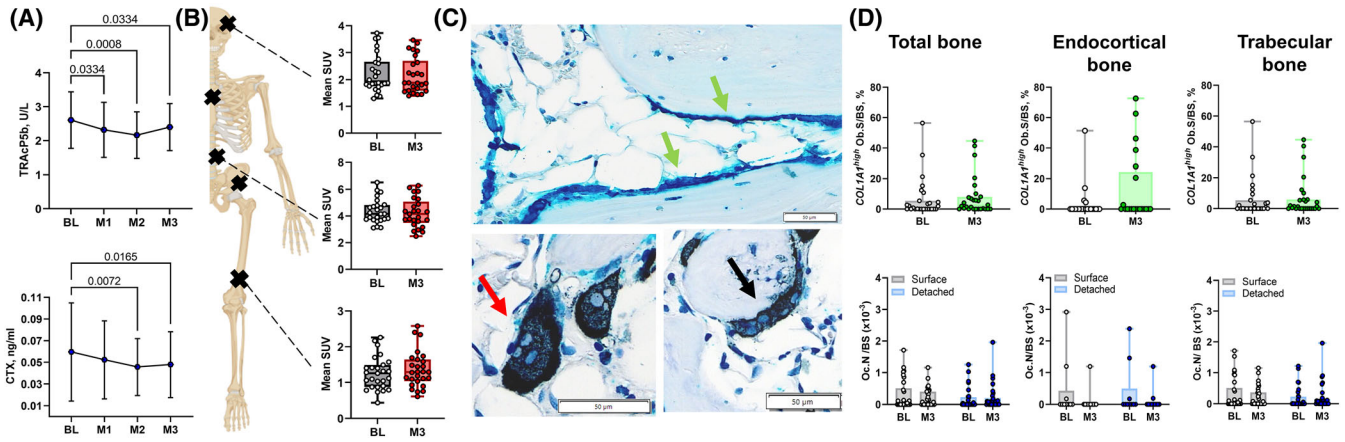

Fig. 1. Effect of ixazomib on serum biomarkers. (*A*) Serum levels of selected biomarkers of bone remodeling and metabolism were measured before and after each 28-day ixazomib cycle for the first three treatment cycles, including tartrate-resistant acid phosphatase 5b (TRACP5b) and C-terminal telopeptide (CTX). TRACP5b two-way ANOVA: $F(3,76) = 4.930$; $p = 0.0035$; CTX two-way ANOVA: $F(3,76) = 3.867$; $p = 0.0125$. (*B*) Mean SUV of skull, sternum, vertebrae, pelvis, and femur were assessed in NaF-PET scans before and after three full 28-day cycles. (*C*, *D*) The percentage of *COL1A1*^{high} osteoblast surface per BS (*COL1A1*^{high} Ob.S/BS) was assessed by in situ hybridization of *COL1A1* in trephine iliac crest bone biopsies collected before and after 3 months of ixazomib treatment. In a representative image of *COL1A1* detection, the *COL1A1*^{high} Ob.S (dark blue) is indicated by green arrows. (*C*, *D*) The number of osteoclast per BS (Oc.N/BS) was assessed by TRACP5b immunostaining; osteoclasts were classified as "detached" when not immediately positioned on BS (red arrowhead) or "surface" if the total osteoclastic (Oc) surface was directly positioned on a BS (black arrowhead). BL = baseline; M1 = month 1; M2 = month 2; M3 = month 3. SUV= standard uptake value.

Short-term ixazomib treatment increases trabecular bone volume in patients with stable MM

The analyses of OPN^{+}-immunostained bone sections revealed a significant increase in trabecular bone volume (BV/TV) in patients with MM patients after three full 28-day ixazomib treatment, compared with baseline (Fig. 2*A*). The ΔBV/TV was nonsignificantly higher in patients with light chain MM (Fig. 2*B*) and independent of number of previous treatment lines (Fig. 2*C*), presence of high-risk translocations (t(4;14), t(14;16) or del17p; Fig. 2*D*), or R-ISS classification (Fig. 2*E*). Multiple linear regression analyses ($R^2 = 0.29$, df = 18) revealed that changes in BV/TV were independent of baseline age, sex, days from stem cell transplantation, and number of previous treatment lines but weakly associated with baseline BMI ($F(1, 18) = 4.655$; β coefficient 1.549 ± 0.718; $p = 0.045$). Regression analyses demonstrated a significant correlation between treatment-induced changes in BV/TV and P1NP, further consolidating the net bone anabolic effect of ixazomib (Fig. 2*F*).

Ixazomib treatment promotes enlarged BSUs

Trabecular bone is composed of microscopic BSUs delimited by OPN^{+} cement lines that represent each individual bone remodeling event. To better understand the bone anabolic effect of ixazomib treatment, all superficial BSU profiles (BSU^{SUP}.Pf.) detected in OPN-immunostained slides were outlined and analyzed. A total of 4673 BSU^{SUP}.Pf. were detected across 56 bone biopsies (18–237 per biopsy) collected from 30 patients with MM before and after three full cycles of ixazomib treatment. Overall, BSU^{SUP}.Pf. volume per tissue volume (BSU^{SUP}.Pf.BV/TV) was significantly increased following ixazomib treatment, compared with baseline (Fig. 3*C*), further supporting the bone anabolic effect of this second-generation PI. Importantly, a significant number of BSU^{SUP}.Pf. was very enlarged (enlarged BSU^{SUP}.Pf.) compared with the regular BSU.Pf. size found in baseline biopsies (Fig. 3*A*,*B*) and other studies.[23] Further examination of BSU^{SUP}.Pf. frequency distribution according to size revealed that after ixazomib treatment, a significant proportion of BSU^{SUP}.Pf. was indeed significantly enlarged, presenting an area ≥200,000 μm^2 (Fig. 3*D*). Moreover, after 3 months of ixazomib treatment, the outlined BSU^{SUP}.Pf. presented significant differences in their relative distribution according to circularity, aspect ratio, and width compared with baseline (Fig. 3*E*), while shape factor and solidity remained unchanged (Fig. S2).

Characterization of enlarged BSU^{SUP}.Pf.

Following the identification of enlarged BSU^{SUP}.Pf. in patients with MM before and after ixazomib treatment, a detailed characterization was conducted to better understand the mechanisms of bone formation following treatment administration. First, the OPN^{+} cement lines of origin of enlarged BSU^{SUP}.Pf. were classified as eroded (scalloped lines cutting through the lamella present underneath) or quiescent (smooth lines parallel to defined lamellar structures). Following this classification, no changes were found in the percentage of eroded/quiescent cement lines of origin of enlarged BSU^{SUP}.Pf. following treatment (Fig. 4*A*). To gain further information on the sequence of bone formative events, large BSU^{SUP}.Pf. were scored as "new BSU^{SUP}.Pf.," "parent BSU^{SUP}.Pf.," or "grandparent BSU^{SUP}.Pf." (containing zero, one, or two subsequent layers of historical bone growth). Following this scoring system, we observed that the majority of enlarged BSU^{SUP}.Pf. were classified as new BSU^{SUP}.Pf., suggesting that they were formed as a direct result of ixazomib treatment (Fig. 4*B*). Moreover, 3 months after ixazomib treatment, a significant proportion of enlarged BSU^{SUP}.Pf. were actively undergoing bone formation, quantified as containing osteoid-covered BSs

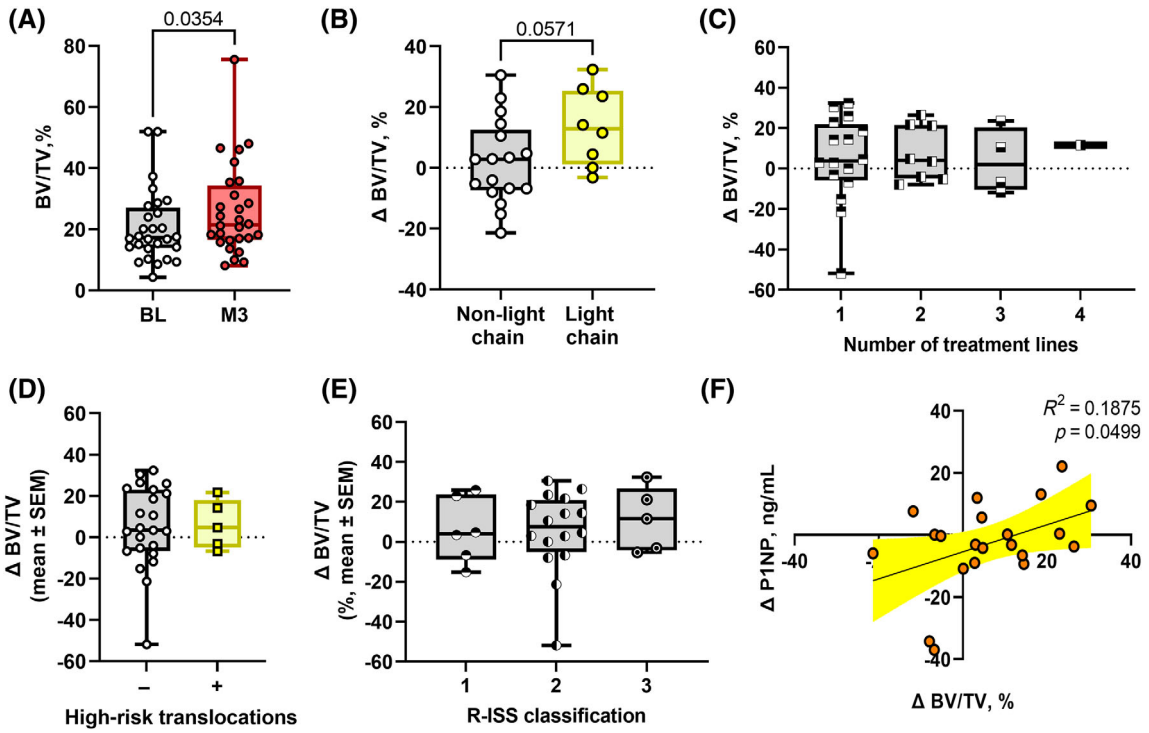

Fig. 2. Effect of ixazomib treatment on trabecular bone volume (BV). (*A*) The trabecular bone volume (BV/TV) was significantly increased after three treatment cycles, as measured on histological sections. Paired Student's *t*-test. (*B*) Patients with light chain MM presented a trend toward higher ΔBV/TV following ixazomib treatment than patients with IgG MM. Unpaired Student's *t*-test. (*C–F*) Changes in BV/TV (ΔBV/TV) were independent of baseline number of previous treatment lines (*C*), presence of high-risk translocations (*D*), or R-ISS classification (*E*). (*F*) Linear correlation between ΔBV/TV and changes in serum P1NP (ΔP1NP) after ixazomib treatment. BL = baseline; M3 = month 3.

(Fig. 4*C*), underscoring the bone anabolic effect of ixazomib. The number of trabecular rods embedded within enlarged BSU^{SUP}.Pf. was quantified (Fig. 4*D*), highlighting the bone anabolic capacity of ixazomib treatment to rejoin trabecular rods. Finally, significantly more enlarged BSU^{SUP}.Pf. contained some degree of woven bone after treatment compared with baseline (Fig. 4*E*).

Discussion

MM remains an incurable hematological cancer with a 5-year survival expectancy of approximately 67% in young patients and 46% in patients age 65–79,[25] and bone osteolysis and pain are hallmarks of the disease.[1,6] Past reports suggested that PIs had a positive bone anabolic effect in MM, but their side effects prevent long-term use in a maintenance setting. In this phase 2 study, we analyzed the effect of the oral, second-generation PI ixazomib on bone resorption and formation in patients with MM in stable remission after the initial 3 months of treatment. Overall, our results support a net bone anabolic effect of ixazomib, which we propose is the result of overflow remodeling-based bone formation and decreased bone resorption.

In this study, we observed a reduction in serum bone resorptive markers CTX[26,27] and TRACP5b[28] upon ixazomib administration. Interestingly, immunohistochemical staining of TRACP5b failed to reveal treatment-induced changes in osteoclast density, suggesting that the number of osteoclasts was unaffected, but their resorptive capacity diminished. All but one patient included in this study also received bisphosphonate treatment, as is the standard of care for MM, which could have directly influenced the results. It has been widely reported that bisphosphonates bind the BS with high affinity and act as osteoclast inhibitors upon their surface attachment and initiated resorption.[29,30] Indeed, osteoclast detachment from BS is a common occurrence in bisphosphonate-treated patients,[31] and this was unaffected by ixazomib. It is likewise possible that bisphosphonate-induced osteoclast inhibition masks part of the osteoclastic effect of ixazomib, which is challenging to investigate by histomorphometry because one can only investigate osteoclast abundance, not their resorptive activity. Still, the reduction in serum CTX and TRACP5b upon ixazomib treatment strongly supports a systemic osteoclastic effect that warrants further investigation.

Despite the fast decrease in bone resorption markers (CTX, TRACP5b), serum markers of bone formation, P1NP and bALP,[27,32,33] remained largely unaffected; however, changes in serum P1NP levels correlated with changes in bone volume, as measured in histological sections. Because bone resorption and formation are tightly coupled events of the bone remodeling process, alterations in serum biomarkers of bone formation generally follow changes in bone resorption markers, which is not the case upon ixazomib treatment. Our data thus suggest that bone formation remains active following ixazomib treatment, even if the treatment reduces osteoclastic bone resorption. One might have expected that the increase in BV/TV would be the result of more drastic changes in the bone resorption and

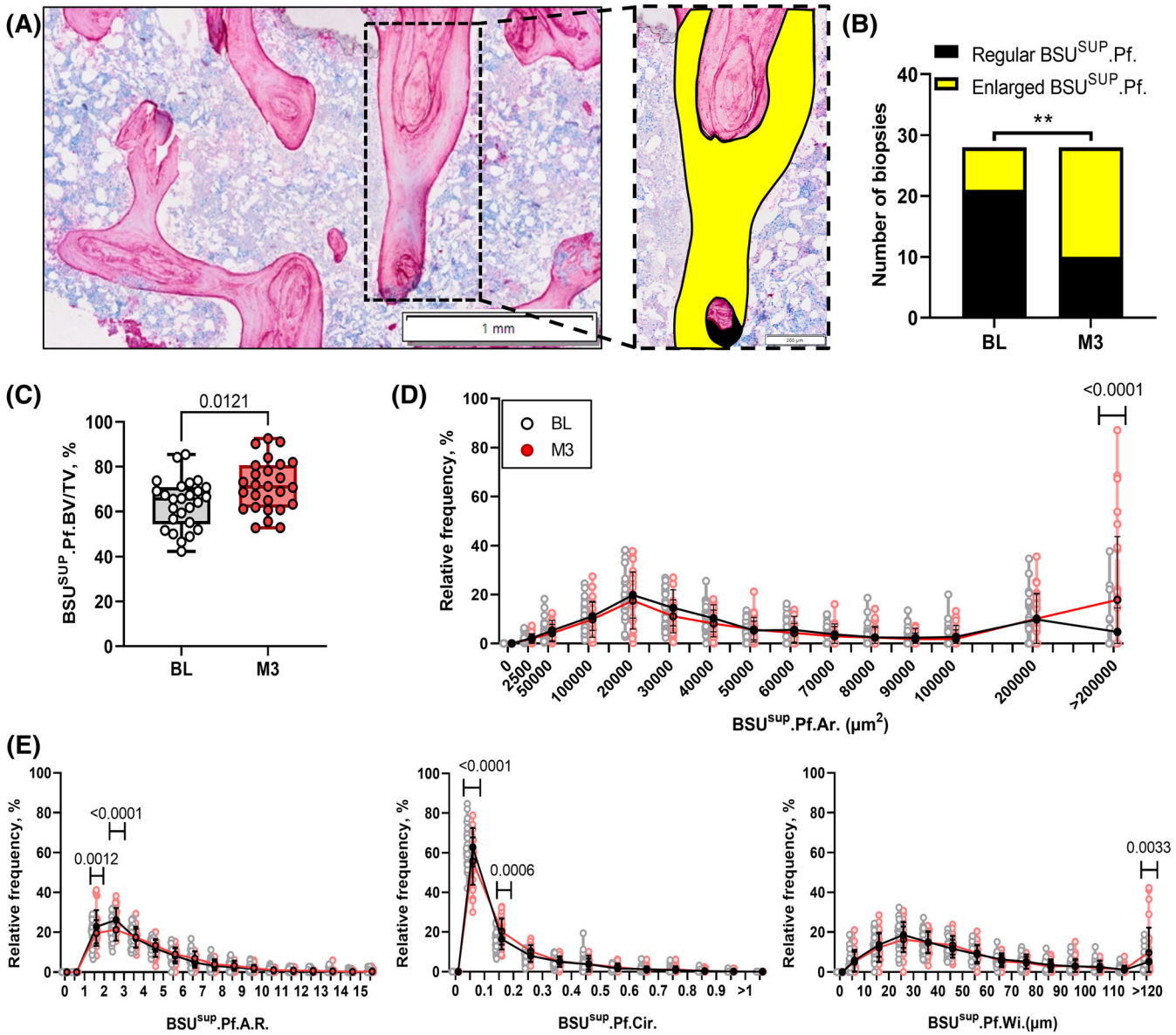

Fig. 3. Effect of ixazomib treatment on BSU^{SUP}.Pf. (*A*) Representative images of OPN^{+} immunostaining defining cement lines in trabecular bone in biopsies from patients with MM included in this study revealed enlarged BSU^{SUP}.Pf. (yellow area) compared to regular sized BSU^{SUP}.Pf. (black area); BSU^{SUP}.Pf. was manually drawn across all bone biopsies for further analyses. (*B*) Bone biopsy distribution before and after ixazomib treatment upon visual classification according to presence of any enlarged BSU^{SUP}.Pf. or regular size BSU^{SUP}.Pf. (*C*) Analyses of BSU^{SUP}.Pf. bone volume per total volume (BSU^{SUP}.Pf.BV/TV) in trabecular bone of patients with MM before and after 3 months of ixazomib treatment. (*D*) Relative distribution analyses of BSU^{SUP}.Pf. in biopsies collected before or after treatment according to area (BSU^{SUP}.Pf.Ar.; two-way ANOVA: $F(14, 810) = 3.548$). (*E*) Relative distribution analyses of BSU^{SUP}.Pf. in biopsies collected before or after treatment according to circularity (BSU^{SUP}.Pf.Cir.; two-way ANOVA: $F(11, 324) = 7.499$), aspect ratio (BSU^{SUP}.Pf.A.R.; two-way ANOVA $F(16,459) = 4.439$), and width (BSU^{SUP}.Pf.Wi.; two-way ANOVA $F(13, 378) = 1.721$). BL = baseline; M3 = month 3.

formation markers, instead of this subtle shift in the balance between bone resorption and formation markers. Consistent P1NP levels over time indeed suggest unchanged incidence of bone formation events, while reduced CTX levels indicate a reduced incidence of bone resorption events, normally considered a prerequisite for coupled bone formation. This implies that the higher BV/TV observed in histological sections may be the result of a maintained cumulative activity of preexisting bone-forming events and the reduced presence of new resorption events. This is further supported by the NaF-PET data, which indicate unchanged bone formation rates. Surprisingly, maximum uptake values at osteolytic lesion sites were significantly lower following treatment, which may also be a consequence of bisphosphonate treatment, since previous studies showed that bisphosphonates inhibited the transition from bone resorption to formation.[34,35]

Our histological results show that ixazomib promotes a significant increase in trabecular bone volume. This bone anabolic effect

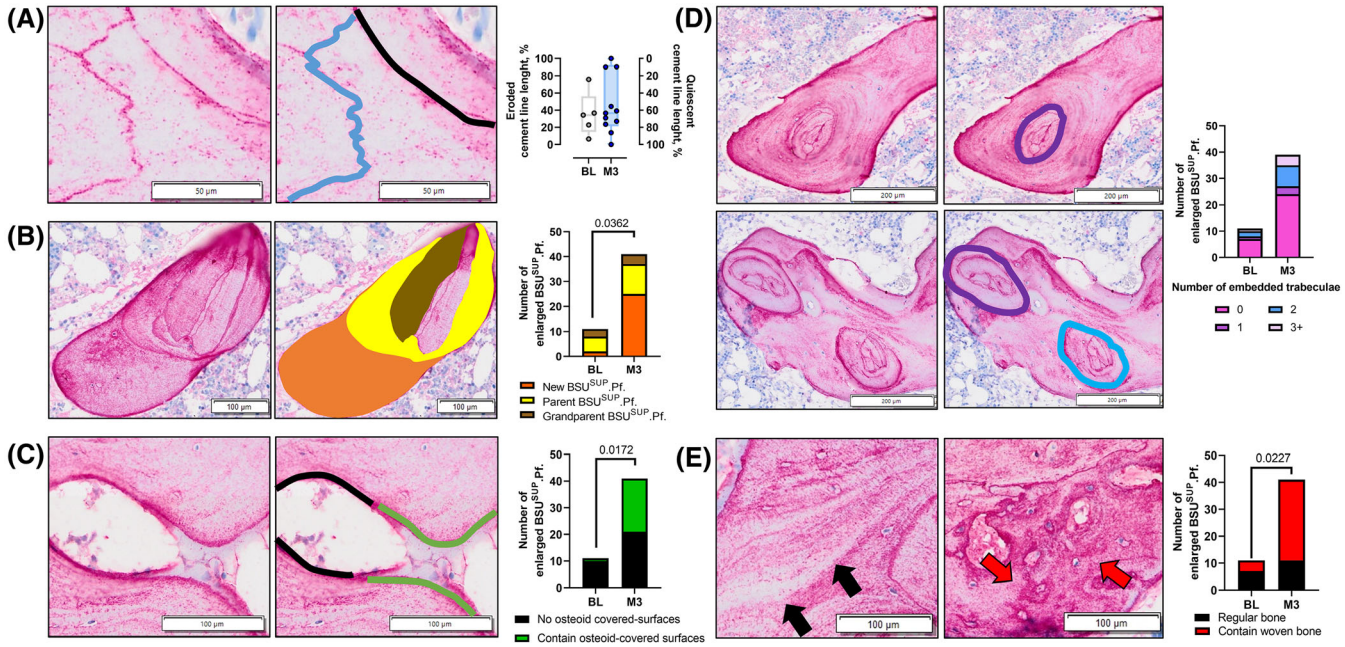

Fig. 4. Characterization of BSU^{SUP}.Pf. ≥200,000 µm^2 (enlarged BSU^{SUP}.Pf.). (*A*) Representative image of bone resorptive surface (blue line) and quiescent BS (black line) and distribution of percentage of cement line length displaying quiescent and resorptive BSs across enlarged BSU^{SUP}.Pf. before and after three full 28-day cycles of ixazomib treatment. (*B*) Representative image of scoring system applied to distinguish sequential bone growth. Enlarged BSU^{SUP}.Pf. were scored as follows: (i) "new BSU^{SUP}.Pf.": presenting no additional layers of bone growth toward marrow (denoted as orange area); (ii) "parent BSU^{SUP}.Pf.": presenting one layer of subsequential bone growth (yellow area); (iii) "grandparent BSU^{SUP}.Pf.": presenting ≥2 layers of superficial bone growth (brown area); enlarged BSU^{SUP}.Pf. were quantified according to their surface score. Chi-squared test = 6.637; df = 2. (*C*) Representative image of an osteoid-covered BS (osteoid-covered surface indicated by green and non-osteoid-covered surface in black) and quantification of enlarged BSU^{SUP}.Pf. presenting any degree of osteoid-covered surfaces. Chi-squared = 5.675; df = 1. (*D*) Enlarged BSU^{SUP}.Pf. were further classified according to the number of embedded trabecular rods; representative images of 1 (purple line in top right image) and 2 (purple and blue lines bottom right image) embedded trabeculae. (*E*) Representative image of an enlarged BSU^{SUP}.Pf. containing regular bone (note organized lamellar structure indicated by black arrows) and woven bone (disorganized bone matrix indicated by red arrows). Quantification of number enlarged BSU^{SUP}.Pf. containing woven bone before and after treatment. Chi-squared = 5.191; df = 1 BL = baseline; M3 = month 3.

was independent of myeloma subtype, R-ISS stage, treatment line, or karyotypic characterization, supporting the effectiveness of treatment independently of myeloma aggressiveness. Similarly, and in contrast to the consensus,[23,36-38] changes in trabecular bone volume were independent of age in this patient population, which can be due to limited sample size or disease-induced alterations in bone volume.

During physiological bone remodeling, different players within a basic multicellular unit (BMU) orchestrate a highly synchronized process that involves physical and temporal coordination. Bone remodeling includes four phases: (i) activation of resorption, (ii) initial bone resorption phase, (iii) a reversal–resorptive phase (Rv.Rs), and (iv) a bone formation phase.[39-42] Bone resorption commences with the recruitment of osteoclast precursors to surfaces prone to undergo remodeling. Here, the precursors fuse to become active multinucleated bone-resorbing osteoclasts, which repeatedly erode the quiescent BS until the final erosion depth is reached during the reversal–resorption phase, and bone formation is initiated. During the bone formation phase,[43] the eroded cavity is filled, forming a BSU. The eroded surfaces embedded below a BSU created during the formation phase can be histologically identified as scalloped/eroded OPN^{rich} cement lines breaking through the lamella situated directly beneath.[23,44,45] If the eroded cavity is overfilled, bone formation may occur, not only on eroded surfaces but also overflowing to adjacent quiescent surfaces, repressting the so-called overflow remodeling-based bone formation.[46] The quiescent surfaces embedded below a BSU are histologically identified as smooth/quiescent OPN^{poor} cement lines running parallel to the lamella situated directly beneath.[23,44] During growth and anabolic treatment, bone formation may also occur directly on quiescent surfaces without prior resorption (modeling-based bone formation).[23,43,44] In this study, we observed an increased abundance of very large BSU^{SUP} (>200,000 µm^2) following ixazomib treatment, along with unchanged osteoblast density. Thus, we propose a model in which ixazomib treatment promotes longer formation events, where an unchanged number of osteoblasts continue laying osteoid for longer periods, ultimately leading to net bone formation (Fig. 5). This is further supported by our findings that approximately 50% of the large BSU^{SUP} presented quiescent cement lines of origin rather than resorptive surfaces, in contrast to previous studies, where bone modeling was shown to be responsible for just 0.5% superficial BSUs in healthy women.[23] According to our model, we speculate that this unexpected increase in quiescent cement lines represents ixazomib-induced overflow bone formation that follows the normal filling of the resorption lacunae.

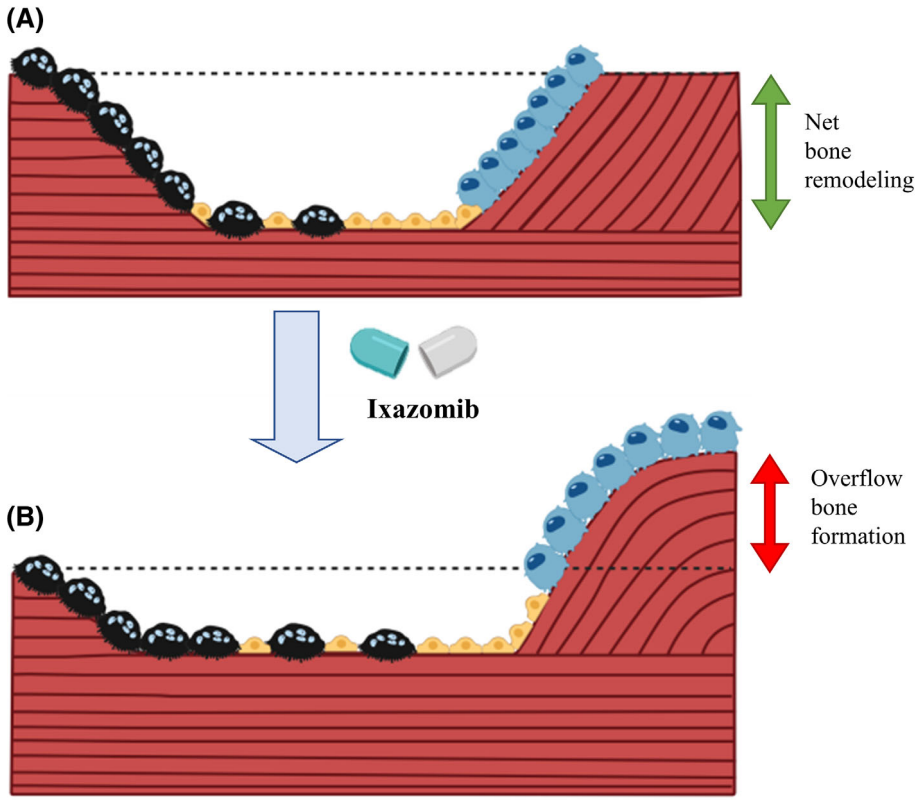

Fig. 5. Graphical representation of our proposed mechanism for ixazomib's net bone anabolic effect. The bone remodeling cycle is spatially and temporally tightly regulated, with osteoclastic (Oc) bone resorption followed by osteoprogenitor/reversal cell (Rv.C) recruitment to the resorption pit. Upon reaching a certain Rv.C threshold, these cells differentiate into osteoblasts, which consequently lay osteoid that will mineralize into new bone; this process leads to unchanged total bone volume (net bone remodeling, *A*). We propose that ixazomib treatment promotes reduced osteoclast activity and longer bone formation events that result in overflow of the resorption pit (bone modeling) and consequent net bone formation (*B*).

Traditional histomorphometric analyses utilize superficial BSU thickness ("wall thickness") as a surrogate marker for recent bone formation[47,48]; here, we took advantage of BSU composition analyses, which we propose as a new tool for studying bone resorption and formation in trabecular bone.[23] Indeed, we previously showed that two-dimensional (2D) analyses of BSU composition directly reflected three-dimensional (3D) microarchitectural parameters independently of sex or skeletal site, with low variability in the frequency of area and width distribution across similarly aged patients.[23] In contrast, our characterization of more than 4500 superficial BSUs revealed treatment-driven changes in area, circularity, width and aspect ratio of superficial BSUs. Overall, our data suggest that ixazomib promotes atypically long bone formation events, and one could argue that the recorded alterations in 2D shape parameters directly reflect 3D changes in trabecular bone volume, as per our previous studies in healthy women of different ages.[23] However, it is important to note the limitations of the study, including its small cohort size, confounding factors (ie, previous and current concomitant treatments), and the limited information that one can gain from 2D histological sections. Moreover, this short-term clinical study did not address a potential rebound effect upon long-term ixazomib treatment or drug discontinuation. Future studies could include long-term follow-up and strategies like tetracycline double labeling to determine the mineral apposition rate, which would substantiate the results presented in this manuscript.

The most striking finding of our analyses was the increase in enlarged superficial BSUs measuring >200,000 μm^2 after just 3 months of ixazomib treatment. Interestingly, a small proportion of enlarged BSUs was also present in baseline biopsies, suggesting a discrete effect of disease or previous treatment lines on BSU^{SUP} area. Importantly, a deeper characterization of these structures revealed that after treatment over 20% of them presented osteoid surfaces, indicating active bone formation sites and suggesting that even larger BSUs would be detectable after longer treatment periods; as no osteoid surfaces were encountered in the baseline large BSU^{SUP}, it can be assumed that ongoing bone formation is a direct consequence of ixazomib treatment. Most of these enlarged structures were completely superficial (ie, classified as new BSU^{SUP}.Pf.) and presented no additional growth layers, further supporting longer bone formation events as a direct consequence of ixazomib treatment and not due to previous treatment lines.

MM is a hematological neoplasia characterized by the development of focal osteolytic lesions, and myeloma bone disease often results in skeletal related events (SREs) that significantly impair overall survival.[49] Bisphosphonate and denosumab treatment are the gold standard for combatting myeloma bone disease in the clinical setting, but each carries its own set of challenges, such as osteonecrosis of the jaw with bisphosphonate treatment or denosumab's rebound effect.[13,14,50-52] Developing double-targeted therapies that function as anticancer medication and contribute to improved bone health is an attainable

future for MM. Here, we demonstrated that a second-generation PI with low side effect prevalence and anticancer properties similar to those of other classes of drugs provides a beneficial bone anabolic effect to patients with stable MM after just 3 months of treatment. Further research will elucidate the exact mechanisms of ixazomib-induced bone formation and its long-term efficacy in a future maintenance setting.

Acknowledgments

The authors would like to thank Malene Hykkelbjerg and Kaja Laursen for their excellent help with this project. This study was partly funded by Takeda Pharmaceutical Company. We also thank the International Myeloma Foundation for its support.

This study was conducted under approval from the Regional Ethical Committee in the Region of Southern Denmark (S-20190043; 04/07/2019) and upon collection of written informed consent. The study is registered at ClincalTrials.gov: NCT0402811. Authors M. Diaz-delCastillo and T.L. Andersen received NIH support, grant AG 075227.

[Correction added on 25 April 2023, after first online publication: the last sentence 'Authors M. Diaz-delCastillo and T.L. Andersen received NIH support, grant AG 075227' has been added]

Author Contributions

Marta Diaz-delCastillo: Conceptualization; methodology; investigation; writing – original draft; data curation. **Michael Tveden Gundesen:** Conceptualization; investigation; writing – original draft; methodology; validation; funding acquisition; data curation. **Christian Walther Andersen:** Investigation; methodology; writing – review and editing. **Anne Lerberg Nielsen:** Investigation; methodology; writing – review and editing. **Hanne Elisabeth Højsgaard Møller:** Writing – review and editing; conceptualization; methodology. **Pernille Just Vinholt:** Investigation; methodology; writing – review and editing. **Jon Thor Asmussen:** Investigation; methodology; writing – review and editing. **Ida Bruun Kristensen:** Conceptualization; investigation; methodology; writing – review and editing. **Charlotte Guldborg Nyvold:** Conceptualization; investigation; writing – review and editing; methodology. **Niels Abildgaard:** Conceptualization; investigation; writing – review and editing; methodology. **Thomas Levin Andersen:** Conceptualization; investigation; writing – review and editing; writing – original draft; methodology; supervision. **Thomas Lund:** Conceptualization; investigation; writing – original draft; writing – review and editing; funding acquisition; methodology; supervision.

Disclosures

NA reports grants from Janssen, Amgen, BMS, Celgene and Takeda, and is on the advisory board of Jansen, BMS and Takeda. The remaining authors have nothing to disclose.

Peer Review

The peer review history for this article is available at https://www.webofscience.com/api/gateway/wos/peer-review/10.1002/jbmr.4807.

Data Availability Statement

The data that support the findings of this study are available on request from the corresponding author. The data are not publicly available due to privacy or ethical restrictions.

References

1. Rajkumar SV, Dimopoulos MA, Palumbo A, et al. International myeloma working group updated criteria for the diagnosis of multiple myeloma. Lancet Oncol. 2014;15(12):e538–e548 Epub 2014/12/03.
2. Lioznov M, El-Cheikh J Jr, Hoffmann F, et al. Lenalidomide as salvage therapy after allo-SCT for multiple myeloma is effective and leads to an increase of activated NK (NKp44(+)) and T (HLA-DR(+)) cells. Bone Marrow Transplant. 2010;45(2):349–353 Epub 20090706.
3. Scott K, Hayden PJ, Will A, Wheatley K, Coyne I. Bortezomib for the treatment of multiple myeloma. The Cochrane database of systematic reviews. 2016;4:Cd010816.
4. Palumbo A, Chanan-Khan A, Weisel K, et al. Daratumumab, bortezomib, and dexamethasone for multiple myeloma. N Engl J Med. 2016;375(8):754–766.
5. Kyle RA, Gertz MA, Witzig TE, et al. Review of 1027 patients with newly diagnosed multiple myeloma. Mayo Clin Proc. 2003;78(1):21–33.
6. Johnsen AT, Tholstrup D, Petersen MA, Pedersen L, Groenvold M. Health related quality of life in a nationally representative sample of haematological patients. Eur J Haematol. 2009;83(2):139–148 Epub 03/05.
7. Horsboel TA, Nielsen CV, Andersen NT, Nielsen B, de Thurah A. Risk of disability pension for patients diagnosed with haematological malignancies: a register-based cohort study. Acta Oncol. 2014;53(6):724–734.
8. Diaz-delCastillo M, Chantry AD, Lawson MA, Heegaard A-M. Multiple myeloma—a painful disease of the bone marrow. Semin Cell Dev Biol. 2021;112:49–58.
9. Roux S, Mariette X. The high rate of bone resorption in multiple myeloma is due to RANK (receptor activator of nuclear factor-kappaB) and RANK ligand expression. Leuk Lymphoma. 2004;45(6):1111–1118.
10. Wada T, Nakashima T, Hiroshi N, Penninger JM. RANKL-RANK signaling in osteoclastogenesis and bone disease. Trends Mol Med. 2006;12(1):17–25.
11. Tian E, Zhan F, Walker R, et al. The role of the Wnt-signaling antagonist DKK1 in the development of osteolytic lesions in multiple myeloma. N Engl J Med. 2003;249(26):2483–2494.
12. Gunn WG, Conley A, Deininger L, Olson SD, Prockop DJ, Gregory CA. A crosstalk between myeloma cells and marrow stromal cells stimulates production of DKK1 and interleukin-6: a potential role in the development of lytic bone disease and tumor progression in multiple myeloma. Stem Cells. 2006;24(4):986–991.
13. Raje N, Terpos E, Willenbacher W, et al. Denosumab versus zoledronic acid in bone disease treatment of newly diagnosed multiple myeloma: an international, double-blind, double-dummy, randomised, controlled, phase 3 study. Lancet Oncol. 2018;19(3):370–381 Epub 20180209.
14. Gonzalez-Rodriguez E, Aubry-Rozier B, Stoll D, Zaman K, Lamy O. Sixty spontaneous vertebral fractures after denosumab discontinuation in 15 women with early-stage breast cancer under aromatase inhibitors. Breast Cancer Res Treat. 2020;179(1):153–159 Epub 20191009.
15. Lloyd AA, Gludovatz B, Riedel C, et al. Atypical fracture with long-term bisphosphonate therapy is associated with altered cortical composition and reduced fracture resistance. Proc Natl Acad Sci U S A. 2017;114(33):8722–8727 Epub 20170731.
16. Zangari M1EDLC, Barlogie B, Elice F, et al. Response to bortezomib is associated to osteoblastic activation in patients with multiple myeloma. Br J Haematol. 2005;131(1):71–73.
17. Terpos E, Heath DJ, Rahemtulla A, et al. Bortezomib reduces serum dickkopf-1 and receptor activator of nuclear factor-kappaB ligand

concentrations and normalises indices of bone remodelling in patients with relapsed multiple myeloma. Br J Haematol. 2006; 135(5):688–692.

18. Lund T, Søe K, Abildgaard N, et al. First-line treatment with bortezomib rapidly stimulates both osteoblast activity and bone matrix deposition in patients with multiple myeloma, and stimulates osteoblast proliferation and differentiation in vitro. Eur J Haematol. 2010; 85(4):290–299.
19. Zangari M, Yaccoby S, Pappas L, et al. A prospective evaluation of the biochemical, metabolic, hormonal and structural bone changes associated with bortezomib response in multiple myeloma. Haematologica. 2011;96(2):333–336.
20. Hurchla M, Garcia-Gomez A, Hornick M, et al. The epoxyketone-based proteasome inhibitors carfilzomib and orally bioavailable oprozomib have anti-resorptive and bone-anabolic activity in addition to anti-myeloma effects. Leukemia. 2013;27(2):430–440.
21. Dimopoulos MA, Gay F, Schjesvold F, et al. Oral ixazomib maintenance following autologous stem cell transplantation (TOURMALINE-MM3): a double-blind, randomised, placebo-controlled phase 3 trial. Lancet. 2019;19(393):253–264.
22. Dimopoulos MA, Špička I, Quach H, et al. Ixazomib as postinduction maintenance for patients with newly diagnosed multiple myeloma not undergoing autologous stem cell transplantation: the phase III TOURMALINE-MM4 trial. J Clin Oncol. 2020;38:4030–4041.
23. Lamarche BA, Thomsen JS, Andreasen CM, Lievers WB, Andersen TL. 2D size of trabecular bone structure units (BSU) correlate more strongly with 3D architectural parameters than age in human vertebrae. Bone. 2022;160:116399 Epub 20220329.
24. Delforge M, Terpos E, Richardson PG, et al. Fewer bone disease events, improvement in bone remodeling, and evidence of bone healing with bortezomib plus melphalan-prednisone vs. melphalan-prednisone in the phase III VISTA trial in multiple myeloma. Eur J Haematol. 2011;86(5):372–384 Epub 20110330.
25. Langseth ØO, Myklebust TÅ, Johannesen TB, Hjertner Ø, Waage A. Incidence and survival of multiple myeloma: a population-based study of 10 524 patients diagnosed 1982–2017. Br J Haematol. 2020;191(3):418–425.
26. Szulc P, Naylor K, Hoyle NR, Eastel R, Leary ET, Project NBHABTM. Use of CTX-I and PINP as bone turnover markers: National Bone Health Alliance recommendations to standardize sample handling and patient preparation to reduce pre-analytical variability. Osteoporos Int. 2017;28(9):2541–2556.
27. Lund T, Abildgaard N, Andersen TL, Delaisse J-M, Plesner T. Multiple myeloma: changes in serum C-terminal telopeptide of collagen type I and bone-specific alkaline phosphatase can be used in daily practice to detect imminent osteolysis. Eur J Haematol. 2010;84(5): 412–420.
28. Terpos E dF, Szydlo R, Hatjiharissi E, Viniou N, Meletis J, et al. Tartrate-resistant acid phosphatase isoform 5b: a novel serum marker for monitoring bone disease in multiple myeloma. Tartrate-resistant acid phosphatase isoform 5b: a novel serum marker for monitoring bone disease in multiple myeloma. Int J Cancer. 2003;106(3): 455–457.
29. Drake MT, Cremers SC. Bisphosphonate therapeutics in bone disease: the hard and soft data on osteoclast inhibition. Mol Interv. 2010; 10(3):141–152.
30. Drake MT, Clarke BL, Khosla S. Bisphosphonates: mechanism of action and role in clinical practice. Mayo Clin Proc. 2008;83(9):1032–1045.
31. Jobke B, Milovanovic P, Amling M, Busse B. Bisphosphonate-osteoclasts: changes in osteoclast morphology and function induced by antiresorptive nitrogen-containing bisphosphonate treatment in osteoporosis patients. Bone. 2014;59:37–43 Epub 20131106.
32. Brunetti GRR, Storlino G, Bortolotti S, et al. LIGHT/TNFSF14 as a new biomarker of bone disease in multiple myeloma patients experiencing therapeutic regimens. Front Immunol. 2018;23(9):2459.
33. Abildgaard N, Glerup H, Rungby J, et al. Biochemical markers of bone metabolism reflect osteoclastic and osteoblastic activity in multiple myeloma. Eur J Haematol. 2000;64(2):121–129.
34. Borggaard XG, Roux JP, Delaisse JM, Chavassieux P, Andreasen CM, Andersen TL. Alendronate prolongs the reversal-resorption phase in human cortical bone remodeling. Bone. 2022;160:116419 Epub 20220410.
35. Jensen PR, Andersen TL, Chavassieux P, Roux J-P, Delaisse J-M. Bisphosphonates impair the onset of bone formation at remodeling sites. Bone. 2021;145:115850.
36. Thomsen JS, Jensen MV, Niklassen AS, Ebbesen EN, Brüel A. Age-related changes in vertebral and iliac crest 3D bone microstructure—differences and similarities. Osteoporos Int. 2015; 26(1):219–228 Epub 20140828.
37. Chen H, Zhou X, Fujita H, Onozuka M, Kubo KY. Age-related changes in trabecular and cortical bone microstructure. Int J Endocrinol. 2013; 2013:213234 Epub 20130318.
38. Macdonald HM, Nishiyama KK, Kang J, Hanley DA, Boyd SK. Age-related patterns of trabecular and cortical bone loss differ between sexes and skeletal sites: a population-based HR-pQCT study. J Bone Miner Res. 2011;26(1):50–62.
39. Abdelgawad ME, Delaisse JM, Hinge M, et al. Early reversal cells in adult human bone remodeling: osteoblastic nature, catabolic functions and interactions with osteoclasts. Histochem Cell Biol. 2016; 145(6):603–615 Epub 20160209.
40. Lassen NE, Andersen TL, Pløen GG, et al. Coupling of bone resorption and formation in real time: new knowledge gained from human Haversian BMUs. J Bone Miner Res. 2017;32(7):1395–1405 Epub 20170228.
41. Andreasen CM, Delaisse JM, van der Eerden BC, van Leeuwen JP, Ding M, Andersen TL. Understanding age-induced cortical porosity in women: the accumulation and coalescence of eroded cavities upon existing Intracortical canals is the main contributor. J Bone Miner Res. 2018;33(4):606–620 Epub 20180104.
42. Andersen TL, Abdelgawad ME, Kristensen HB, et al. Understanding coupling between bone resorption and formation: are reversal cells the missing link? Am J Pathol. 2013;183(1):235–246 Epub 2013/06/12.
43. Langdahl B, Ferrari S, Dempster DW. Bone modeling and remodeling: potential as therapeutic targets for the treatment of osteoporosis. Ther Adv Musculoskelet Dis. 2016;8(6):225–235.
44. Frost M, Rahbek E, Ejersted C, et al. Modeling-based bone formation transforms trabeculae to cortical bone in the sclerotic areas in Buschke-Ollendorff syndrome. A case study of two females with LEMD3 variants. Bone. 2020;135:115313.
45. Andersen TL, Delaisse J-M, Thomsen JS, Andreasen CM. Significance of reversal-resorption phase in bone loss. Osteoporotic Fracture and Systemic Skeletal Disorders. Singapore: Springer; 2022 pp 101–110.
46. Rooney AM, Dempster DW, Nieves JW, Zhou H, Bostrom MP, Cosman F. Effects of teriparatide and loading modality on modeling-based and remodeling-based bone formation in the human femoral neck. Bone. 2022;157:116342.
47. Dempster DW, Arlot MA, Meunier PJ. Mean wall thickness and formation periods of trabecular bone packets in corticosteroid-induced osteoporosis. Calcif Tissue Int. 1983;35(4–5):410–417.
48. Kragstrup J, Melsen F, Mosekilde L. Thickness of bone formed at remodeling sites in normal human iliac trabecular bone: variations with age and sex. Metabolic bone disease and related. Research. 1983;5(1):17–21.
49. Kim C, Bhatta S, Cyprien L, Fonseca R, Hernandez RK. Incidence of skeletal-related events among multiple myeloma patients in the United States at oncology clinics: observations from real-world data. J Bone Oncol. 2018;14:100215.
50. Pozzi S, Raje N. The role of bisphosphonates in multiple myeloma: mechanisms, side effects, and the future. Oncologist. 2011;16(5): 651–662.
51. Vargas-Franco JW, Castaneda B, Rédiní F, Gómez DF, Heymann D, Lézot F. Paradoxical side effects of bisphosphonates on the skeleton: what do we know and what can we do? J Cell Physiol. 2018;233(8): 5696–5715.
52. Anastasilakis AD, Makras P, Yavropoulou MP, Tabacco G, Naciu AM, Palermo A. Denosumab discontinuation and the rebound phenomenon: a narrative review. J Clin Med. 2021;10(1):152.